ACS OMEGA

http://pubs.acs.org/journal/acsodf

Article

New Anti-Inflammatory β-Resorcylic Acid Lactones Derived from an Endophytic Fungus, *Colletotrichum* sp.

Jaekyeong Kim,[⊥] Ji Yun Baek,[⊥] Sunghee Bang,[⊥] Ji-Young Kim, Yeongwoon Jin, Jin Woo Lee, Dae Sik Jang, Ki Sung Kang,* and Sang Hee Shim*

Cite This: *ACS Omega* 2023, 8, 3530−3538

Read Online

ACCESS | Metrics & More | Article Recommendations | Supporting Information

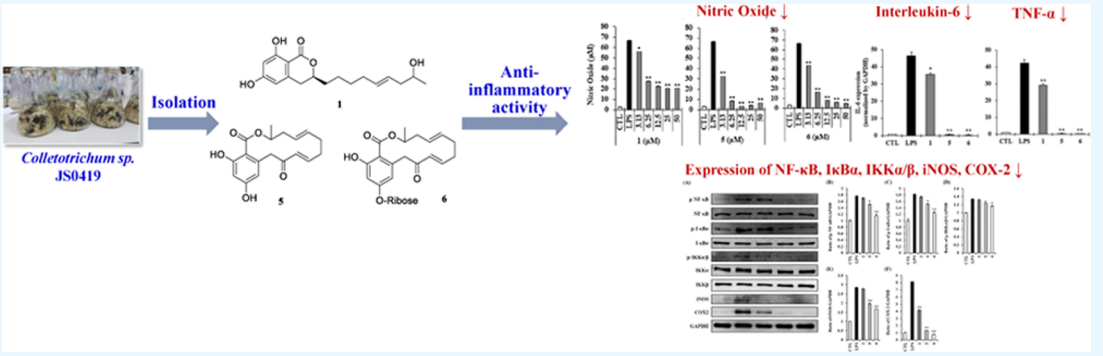

ABSTRACT: The endophytic fungus *Colletotrichum gloeosprioides* JS0419, isolated from the leaves of the halophyte *Suaeda japonica*, produced four new β-resorcylic acid derivatives, colletogloeopyrones A and B (**1** and **2**) and colletogloeolactones A and B (**3** and **4**), and seven known β-resorcylic acid lactones (RALs). The structures of these compounds were elucidated via analysis of the high-resolution mass spectrometry and nuclear magnetic resonance data. Compounds **1** and **2** showed a dihydrobenzopyranone ring with a linear C9 side chain, which is rarely observed in RALs. All isolated compounds were evaluated for their anti-inflammatory activities. Colletogloeopyrone A (**1**), monocillin II (**5**), and monocillin II glycoside (**6**) were effective in reducing nitric oxide production without cytotoxicity. They also inhibited the secretion of interleukin-6 (IL-6) and tumor necrosis factor-α (TNF-α), as demonstrated by the expression of mRNA corresponding to IL-6 and TNF-α. Mechanistically, compounds **5** and **6** significantly inhibited the protein expression of nuclear factor-κB, IκBα, IKKα/β, inducible nitric oxide synthase, and cyclooxygenase (COX)-2, whereas compound **1** only inhibited COX-2 expression. This study indicated that RAL-type compounds **1**, **5**, and **6** demonstrated potential anti-inflammatory activity by inhibiting the synthesis of pro-inflammatory cytokines.

INTRODUCTION

Endophytes live inside plants for a part of their life cycle and produce biologically active metabolites in association with their hosts.[1] β-Resorcylic acid lactones (RALs) are produced by endophytes. RALs are a class of fungal polyketide metabolites comprising a β-resorcylic acid unit (2,4-dihydroxy-benzoic acid) embedded in a 14-membered lactone.[2] RAL-type compounds exhibit extensive biological activities, including antifungal, cytotoxic, antimalarial, antiviral, antiparasitic, nematicidal, estrogenic, protein tyrosine kinase, and ATPase inhibition.[3−6] This has led to significant interest in these compounds in the field of natural product chemistry. To discover new bioactive compounds in endophytes, we investigated the chemical profiles of halophyte-associated endophytic fungal extracts using liquid chromatography−mass spectrometry (LC−MS). The fungal strain JS0419 of *Colletotrichum gloeosporioides* isolated from the plant *Suaeda japonica* was selected because it produces a variety of secondary metabolites with unique ultraviolet (UV) patterns. After fermentation and subsequent purification, *C. gloeosporioides* JS0419 was found to produce two distinctive classes of compounds, cyclic lipodepsipeptides and polyketides, as published by our group before.[7,8] Further chemical investigations demonstrated new polyketides with RAL skeleton with potent anti-inflammatory activities (Figure 1). In this study, we report the isolation, structure elucidation, and anti-inflammatory activities of these compounds.

RESULTS AND DISCUSSION

Isolation and Structure Elucidation. Four new (**1**−**4**) and seven known (**5**−**11**) polyketides were isolated from

Received: December 14, 2022
Accepted: January 4, 2023
Published: January 12, 2023

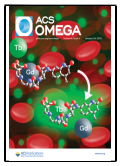

https://doi.org/10.1021/acsomega.2c07962
ACS Omega 2023, 8, 3530−3538

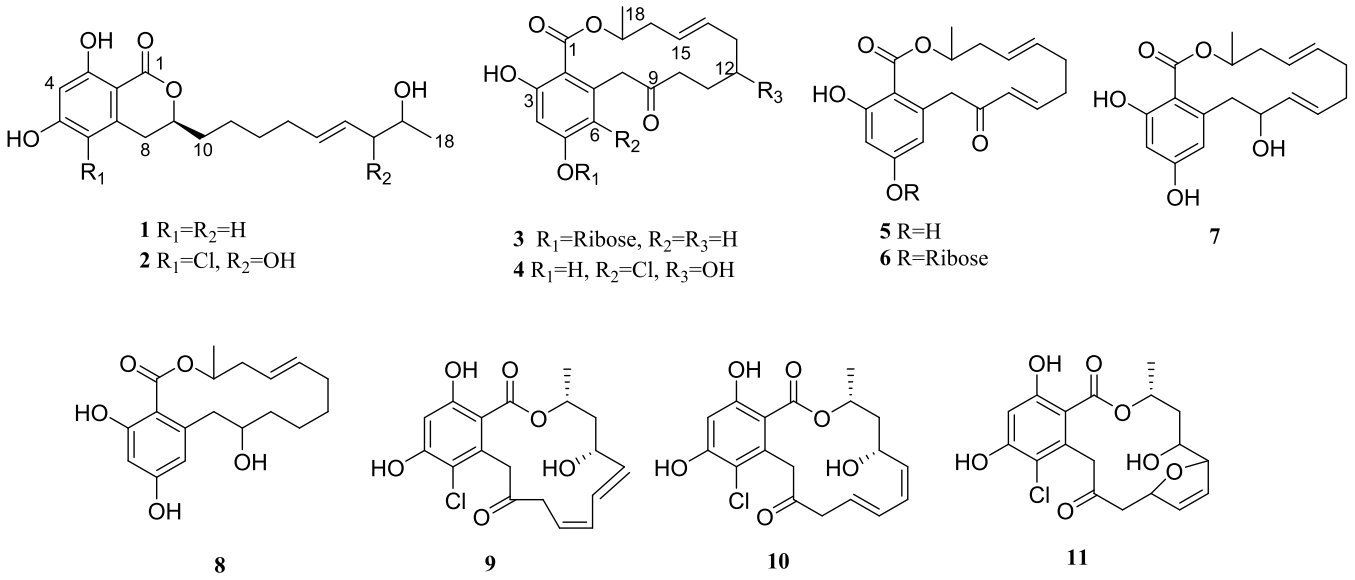

Figure 1. Structures of the isolated compounds (**1**−**11**).

cultures of *C. gloeosporioides* JS419 (Figure 1). Upon comparison of the spectral data with those available in the literature, the known compounds were identified as monocillin II (**5**),[3] monocillin II glycoside (**6**),[3] 10α-hydroxy monocillin II (**7**),[4] (5*E*)-3,4,7,8,9,10,11,12-octahydro-11,14,16-trihydroxy-3-methyl-1*H*-2-benzoxacyclotetradecin-1-one (**8**),[4] pochonin L (**9**),[5] monorden analogue-1 (**10**),[6] and radicicol D (**11**).

The molecular formula of compound **1**, named colletogloeopyrone A, was determined to be $C_{18}H_{24}O_5$ based on the HRESIMS data (observed $[M + Na]^+$ *m*/*z* 343.1519, calculated $[M + Na]^+$ *m*/*z* 343.1516) with seven degrees of unsaturation. Since its ^{13}C NMR spectrum showed nine sp^2 carbons corresponding to four double bonds and a carboxylic group, it must be a bicyclic compound to meet the unsaturation criterion gleaned from the molecular formula (Table 1). The presence of β-resorcylic acid (2,4-dihydroxybenzoic acid) was deduced from the *meta*-coupled proton signals (J = 2.0 Hz) and the carboxylic carbon signal. Interpretation of $^1H-^1H$ COSY allowed the assignment of $CH_2-CH(O)-CH_2-CH_2-CH_2-CH_2-CH=CH-CH_2-CH(O)-CH_3$ corresponding to C-8 to C-18, and its connection with the β-resorcylic acid moiety was confirmed by the heteronuclear multiple bond correlation (HMBC) spectrum (Figure 2). The HMBCs of the methylene protons H_2-8 and the oxymethine proton H-9 at δ_H 4.51 allowed connection of the long chain with the aromatic ring. Characteristically, oxymethine (C-9) was linked to C-1 through an ester linkage based on strong HMBCs with C-7 (δ_C 143.7) of the aromatic ring and carboxylic carbon, forming a benzopyranone ring. Thus, a planar structure was established as shown in the figure. Although it was difficult to assign the geometry of the double bond at C-14 and C-15 by coupling constants because of the overlapping proton NMR signals, it was assigned as trans (*E*) based on the ^{13}C resonances of C-13, 14, and 15.[9] The absolute stereochemistry of C-9 was tentatively assigned to be *S* by comparison of its optical rotation with those in the reference. 6-Hydroxymellein with 9*S* showed positive optical rotations, whereas 6-hydroxymellein with 9*R* showed negative values. Unfortunately, C-17 bearing a hydroxyl group could not be determined because the isolated amount was not sufficient for the modified Mosher's reaction.[10] Therefore, we tried a quantum mechanics-based computational analysis using DP4 statistical calculation.[11−14] Two possible isomers with 17*S* and 17*R* configurations were calculated, in result, one isomer with 17*S* has 87.9% of probability over the other isomer with 17*R* (Table S3). Thus, it was hard to define the absolute stereochemistry based on the quantum mechanics-based calculations.

Table 1. ^1H and ^{13}C NMR Data for Compounds 1 and 2 in CD_3OD

	1		2	
no.	δ_C, type[b]	δ_H (J in Hz)[a]	δ_C, type[b]	δ_H (J in Hz)[a]
1	171.8		171.5	
2	101.7		102.3	
3	165.7		164.0	
4	102.3	6.19 (d, 2.5)	103.1	6.37 (s)
5	166.4		162.5	
6	108.1	6.22 (d, 2.5)	113.3	
7	143.7		140.3	
8	34.1	2.89 (dd, 16.0, 4.0)	31.9	3.24 (dd, 17, 3.0)
		2.83 (dd, 16.0, 11.0)		2.79 (dd, 17, 12)
9	80.9	4.51 (m)	80.2	4.54 (m)
10	35.8	1.81 (m)	35.8	1.86 (m)
		1.72 (m)		1.80 (m)
11	25.6	1.58 (m)	25.6	1.61 (m)
		1.49 (m)		1.51 (m)
12	30.5	1.44 (m)	30.2	1.51 (m)
13	33.7	2.06 (m)	33.5	2.14 (m)
14	133.9	5.46 (m)	134.3	5.71 (dt, 16, 7.0)
15	128.1	5.49 (m)	131.0	5.55 (ddt, 16, 7.0, 1.5)
16	43.6	2.18 (m)	78.0	3.85 (dd, 7.0, 5.0)
		2.10 (m)		
17	68.8	3.73 (m)	71.8	3.66 (qd, 6.5, 5.0)
18	23.0	1.13 (d, 6.0)	18.8	1.13 (d, 6.5)

[a]Measured at 500 MHz. [b]Measured at 125 MHz.

Compound **2**, named colletogloeopyrone B, was also isolated as a yellowish amorphous solid, and its MS showed a molecular ion cluster at *m*/*z* 393/395 in a ratio of 3:1, indicative of the presence of one chlorine atom. The molecular formula of **2** was determined as $C_{18}H_{23}ClO_6$ by HRESIMS analysis (observed $[M + Na]^+$ *m*/*z* 393.1078, calculated $[M + Na]^+$ *m*/*z* 393.1075).

https://doi.org/10.1021/acsomega.2c07962
ACS Omega 2023, 8, 3530−3538

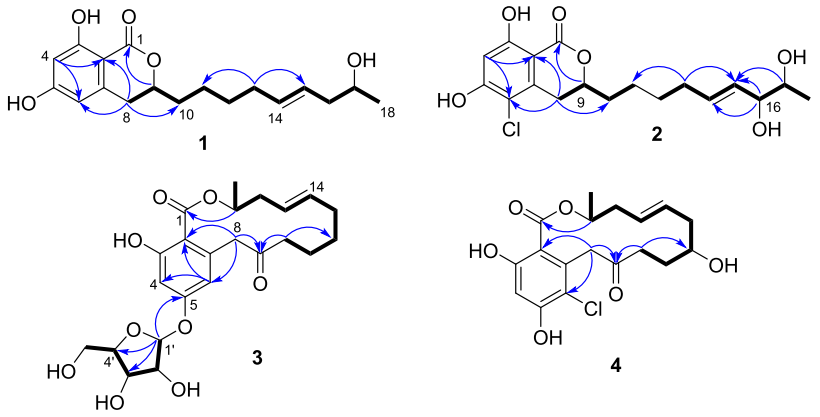

Figure 2. $^{1}H-^{1}H$ COSY, key heteronuclear multiple bond correlation (HMBC) of compounds **1**−**4**.

The structure of **2** was analogous to **1** based on a similar UV pattern (λ_{max} = 218 nm) and NMR. However, only one singlet aromatic proton appeared in **2** unlike **1**, suggesting an additional substituent on the aromatic ring (Table 1). In addition, compound **2** had an additional oxymethine group compared to compound **1**. Position C-6 was deduced to be chlorinated based on its chemical shift and the HMBCs of C-6 with the singlet aromatic proton and H_2-8. In addition, careful analysis of the $^{1}H-^{1}H$ COSY spectrum revealed the presence of a 1,2-diol group connected by a double bond, whose position was also confirmed by HMBCs. Strong HMBCs of the terminal methyl doublet protons with two oxymethine carbons and of the oxymethine protons with the double-bond carbons indicated that the additional hydroxyl group was attached to C-16 of the long chain compared to that in compound **1**. The geometry of the double bond in **2** was apparently *trans* based on the coupling constant (16 Hz). The absolute stereochemistry of C-9 was also tentatively assigned to be *S* based on the optical rotation. Chemical reactions to establish the absolute configuration of C-16 and C-17 could not be performed due to the limited amount of sample.

Compound **3** (colletogloeolactone A), with the molecular formula of $C_{23}H_{30}O_9$ was also a *β*-resorcylic acid derivative with an aliphatic chain. Signals for *β*-resorcylic acid and an olefinic group were observed in the NMR spectra (Table 2). In addition, characteristic resonances for a pentose [(δ_H 5.67, δ_C 101.8; δ_H 4.19, δ_C 73.6; δ_H 4.09, δ_C 71.2; δ_H 4.11, δ_C 88.1; δ_H 3.70 and 3.64, δ_C 63.3)] were observed in NMR. The pentose was confirmed to be ribose by comparing its NMR resonances with those of the references.[15] We confirmed the location of the ribose by an HMBC from the anomeric proton at δ_H 5.67 with C-5 (δ_C 162.8). The ribose moiety was in an *α* configuration based on the coupling constant of the anomeric proton ($^{3}J_{HH}$ = 4.5 Hz).[15] An isolated methylene moiety appeared at δ_H 4.28 and 3.67 (each 1H, d, *J* = 18 Hz). HMBCs of the methylene protons at δ_H 4.28 and 3.67 (H_2-8) with the aromatic carbons C-2, C-6, and C-7, together with the ketone carbon, indicated the presence of a ketone group at C-9. Upon interpretation of the $^{1}H-^{1}H$ COSY spectrum, the double bond was observed at C-14 and C-15. A strong HMBC of the methyl-bearing oxymethine proton with the carboxylic carbon C-1 suggested that the 14-membered lactone was embedded in *β*-resorcylic acid, as observed in well-known RAL-type compounds, radicicols, and monocillins. The low-field-shifted methine proton at δ_H 5.29 also supported the formation of a 14-membered lactone ring. Finally, the ribose was confirmed to be attached at C-5 based on the HMBC of the anomeric proton H-1′ (δ_H 5.67) with C-5 (δ_C 162.8).

Table 2. ^{1}H and ^{13}C NMR Data for Compounds 3 and 4 in CD_3OD

	3		4	
No.	δ_C, type[b]	δ_H (J in Hz)[a]	δ_C, type[b]	δ_H (J in Hz)[a]
1	172.0		171.3	
2	109.4		109.3[c]	
3	165.5		163.1	
4	104.3	6.65 (d, 2.5)	104.0	6.45 (s)
5	162.8		159.6	
6	114.3	6.47 (d, 2.5)	116.4	
7	140.0		137.1	
8	50.7	4.28 (d, 18.0)	47.2	4.39 (d, 18.0)
		3.67 (d, 18.0)		4.10 (d, 18.0)
9	210.7		209.0	
10	42.0	2.52 (t, 6.5)	39.4	2.69 (ddd, 19.0, 9.0, 2.5)
				2.57 (dt, 19.0, 6.0)
11	23.4	1.62 (m)	31.9	1.83 (m)
12	26.7	1.52 (m)	70.3	3.71 (m)
13	33.6	2.09 (m)	42.6	2.39 (m)
				2.16 (dd, 9.0, 4.5)
14	135.8	5.47 (m)	131.4	5.51 (dd, 7.0, 5.0)
15	126.6	5.47 (m)	128.3	5.56 (m)
16	38.8	2.55 (m)	38.9	2.50 (ddd, 15.0, 7.0, 3.5)
		2.30 (m)		2.33 (m)
17	74.3	5.29 (m)	74.1	5.33 (m)
18	19.5	1.37 (d, 6.5)	19.3	1.37 (d, 6.5)
1′	101.8	5.67 (d, 4.5)		
2′	73.6	4.19 (dd, 6.5, 4.5)		
3′	71.2	4.09 (dd, 6.5, 3.5)		
4′	88.1	4.11 (m)		
5′	63.3	3.70 (dd, 13.0, 3.0)		
		3.64 (dd, 13.0, 4.0)		

[a]Measured at 500 MHz. [b]Measured at 125 MHz.

The molecular formula of compound **4** was established as $C_{18}H_{20}ClO_6$ by HRESIMS in the negative mode. Comparison of its ^{1}H and ^{13}C NMR data with those of compound **3** showed that compound **4** had a chlorinated *β*-resorcylic acid and one oxymethine group in the lactone ring but lacked ribose (Table 2). Upon interpretation of $^{1}H-^{1}H$ COSY and HMBCs, the positions of the chlorination and oxymethine groups were confirmed. To establish the absolute configurations of C-12 and

https://doi.org/10.1021/acsomega.2c07962
ACS Omega 2023, 8, 3530−3538

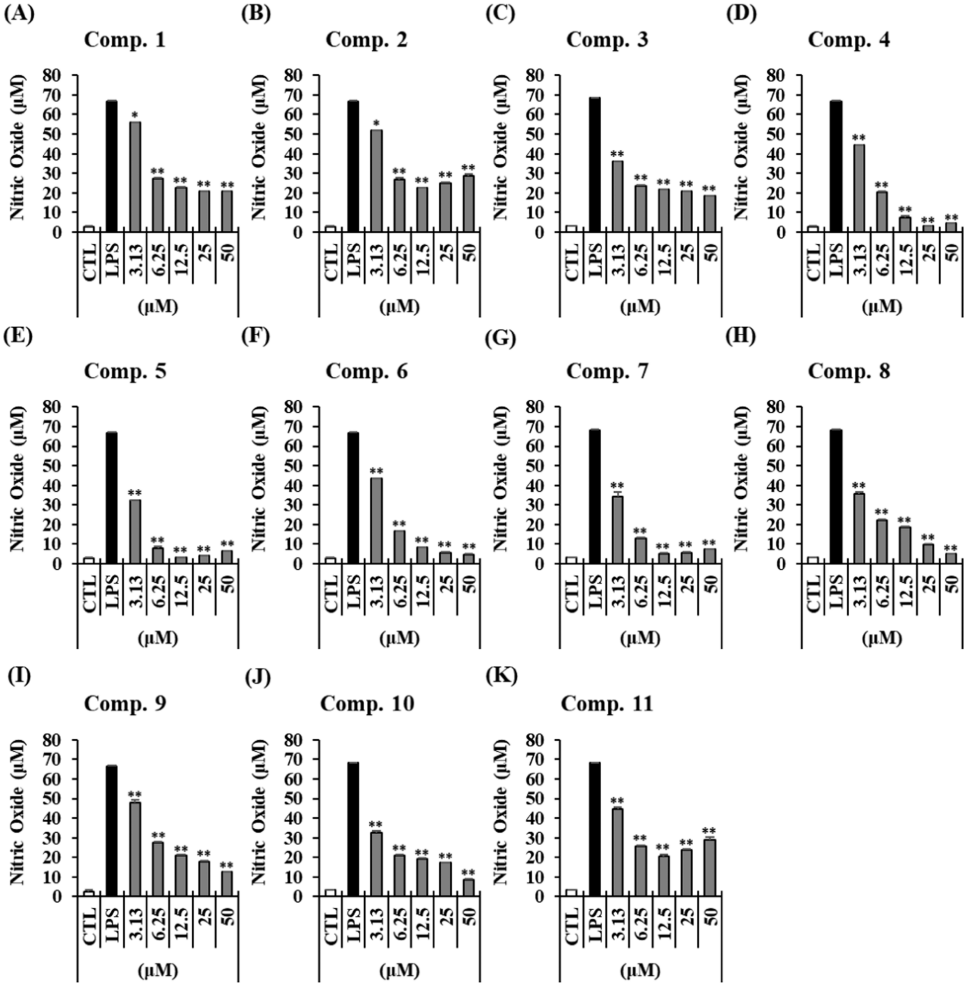

Figure 3. Effects of compounds **1**−**11** on the nitric oxide (NO) production in RAW 264.7 mouse macrophages treated with lipopolysaccharide (LPS). The experiments were conducted in triplicate. (A−K) Effects of compounds **1**−**11** and NO synthase inhibitor on RAW 264.7 mouse macrophages treated with LPS were investigated (mean ± SD, *p < 0.05, **p < 0.01 compared to the group treated with 1 μg/mL of LPS alone).

C-17 in **4**, the quantum mechanics-based computational analysis using DP4 was performed. Four possible isomers (12*R* and 17*R*; 12*R* and 17*S*; 12*S* and 17*R*; 12*S* and 17*S*) were calculated, in result, one isomer with 12*R* and 17*R* and another isomer with 12*S* and 17*S* had 38.3 and 61.7% probabilities, respectively (Table S4). Compound **4** possibly had the same absolute configurations at C-12 and C-17, but it was also hard to define them based on relatively low values of probability on DP4 analysis.

A cell viability assay was conducted to determine the nontoxic concentrations of compounds **1**−**11** in RAW 264.7 cells. Compounds **4**, **5**, **7**, and **8** were weakly cytotoxic, as cell survival reduced to less than 80% at concentrations of 12.5, 25, 12.5, and 25 μM, respectively (Supporting Figure S25). The anti-inflammatory effects of these compounds were assessed at nontoxic concentrations. The inhibitory effect of compounds **1**−**11** on NO production was examined. All compounds reduced nitrite concentration (Figure 3) compared to those observed in the lipopolysaccharide (LPS) control group (66.57 ± 0.49). In particular, co-treatment with compounds **5** and **6** together with LPS showed the lowest NO production of 3.13 ± 0.00 and 4.74 ± 4.74 μM at 12.5 and 50 μM concentrations, and the new compound (**1**) was more effective in inhibiting nitrite production than compound (**2**) with similar structure. These results indicate that compounds **1**, **5**, and **6** may demonstrate anti-inflammatory activity in LPS-activated RAW 264.7 cells.

Secretion of IL-6 increased after treatment with LPS in cells and then decreased upon treatment with 12.5 and 50 μM **5** and **6**, respectively. TNF-α secretion was also significantly inhibited upon treatment with compounds **1**, **5**, and **6** compared to that in the LPS alone treatment group. As a result, compound **1** was effective in inhibiting TNF-α secretion at a concentration of 50 μM, and compounds **5** and **6** were effective in inhibiting IL-6 and TNF-α (Figure 4).

In addition, the mRNA expression of IL-6 and TNF, which are involved in NO and cytokine production, was analyzed. The LPS-mediated increase in the mRNA expression of IL-6 and TNF was significantly inhibited by treatment with compounds **1**, **5**, and **6**. The inhibitory effects of compounds **5** and **6** were stronger than the effect of compound **1**, which showed a pattern similar to that of cytokine secretion (Figure 5).

Western blot analysis was conducted to investigate the effects of compounds **1**, **5**, and **6** on the protein levels of NF-κB, IκBα, and IKKα/β and to examine the inhibition of the expression of pro-inflammatory factors iNOS and COX-2. As shown in Figure 6, when stimulated with LPS alone (1 μg/mL) for 24 h, the protein expression of NF-κB, IκBα, and IKKα/β increased, whereas it was suppressed after treatment with compounds **5** and **6**. In addition, the increase in the protein expression of

https://doi.org/10.1021/acsomega.2c07962
ACS Omega 2023, 8, 3530−3538

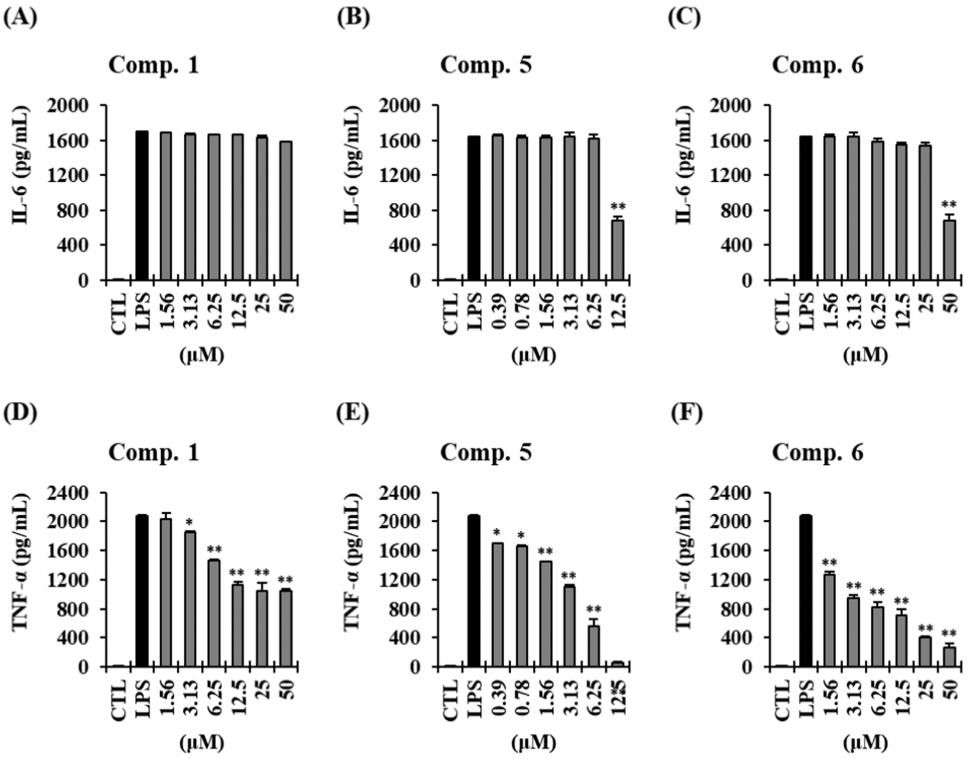

Figure 4. Effect of compounds **1**, **5**, and **6** on interleukin (IL)-6 and tumor necrosis factor (TNF)-α secretion in lipopolysaccharide (LPS)-stimulated RAW 264.7 cells. RAW 264.7 cells were treated with various concentrations of compounds **1**, **5**, and **6** for 2 h and subsequently with LPS (1 μg/mL) for 22 h. (A−C) IL-6 and (D−F) TNF-α concentrations were measured using enzyme-linked immunosorbent assay (ELISA) (mean ± SD, *p < 0.05, **p < 0.01 compared to the group treated with 1 μg/mL of LPS alone).

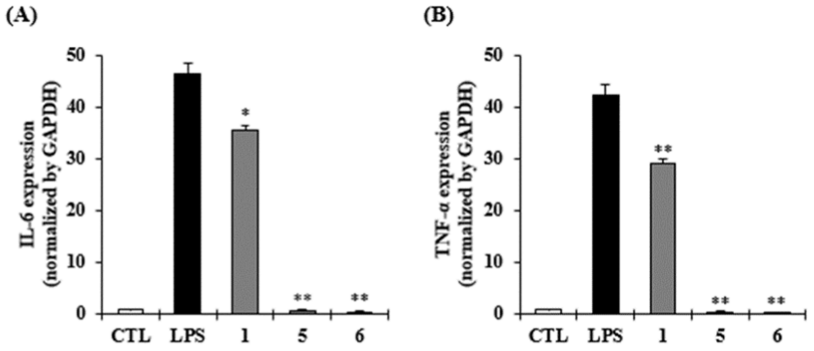

Figure 5. Effect of compounds **1**, **5**, and **6** on interleukin (IL)-6 and tumor necrosis factor (TNF)-α mRNA expression in lipopolysaccharide (LPS)-stimulated RAW 264.7 cells. RAW 264.7 cells were treated with compounds **1** (50 μM), **5** (12.5 μM), and **6** (50 μM) for 2 h and subsequently with LPS (1 μg/mL) for 4 h. (A, B) IL-6 and TNF-α mRNA levels were measured using quantitative reverse transcription-polymerase chain reaction (qRT-PCR) (mean ± SD, *p < 0.05, **p < 0.01 compared to the group treated with 1 μg/mL of LPS alone).

iNOS and COX-2 following LPS stimulation was significantly inhibited by compounds **5** and **6**. Compound **1** was effective only at inhibiting COX-2 expression at a concentration of 50 μM.

CONCLUSIONS

Four new β-resorcylic acid lactones (**1**−**4**), together with seven known ones (**5**−**11**), were isolated from the cultures of the endophytic fungus *Colletotrichum gloeosprioides*. The structures of these compounds were elucidated using high-resolution mass spectrometry (HRMS) and NMR analyses. Compounds **1** and **2** were named colletogloeopyrones A and B. These compounds demonstrated dihydrobenzopyranone ring with a linear C9 side chain. The efforts to establish the absolute configurations using quantum mechanics-based computational analysis using DP4 statistical calculation were made. However, this approach did not provide definitive results. Although most of RALs are β-resorcylic acids embedded in a 14-membered lactone system, to our knowledge, only two precedents for a dihydrobenzopyranone ring with a long aliphatic side chain are cladosporin, an antimalarial agent and penicisimpins.[16,17] Compounds **3** and **4**, named colletogloeolactones A and B, respectively, are β-resorcylic acid compounds fused with a 14-membered lactone. Colletogloeopyrone A (**1**), monocillin II (**5**), and monocillin II glycoside (**6**) significantly decreased NO production but did not show cytotoxicity at concentrations of 6.25, 12.5, and 25 μM, which prompted us to perform additional mechanical experiments. Macrophages stimulated by LPS produce TNF-α, which induces the production of IL-6, amplifying the inflammatory response.[18] Our investigation showed that compounds **1**, **5**, and

https://doi.org/10.1021/acsomega.2c07962
ACS Omega 2023, 8, 3530−3538

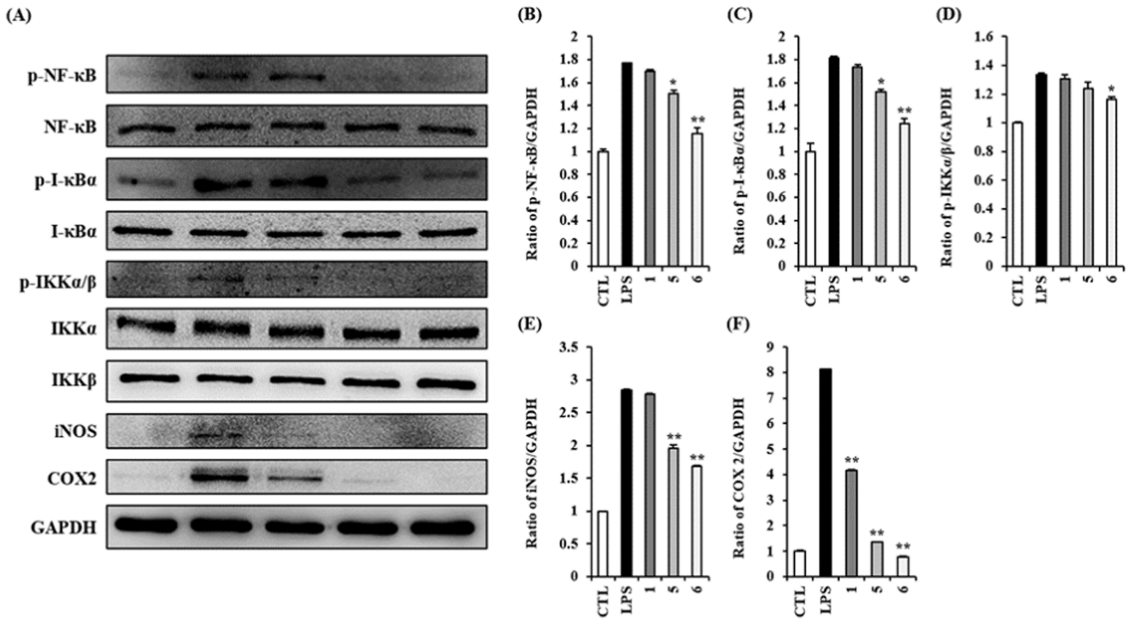

Figure 6. Effects of compounds **1**, **5**, and **6** on the lipopolysaccharide (LPS)-induced expression of nuclear factor (NF)-κB p65, I-κBα, IKKα/β, inducible nitric oxide synthase (iNOS), and cyclooxygenase (COX)-2 proteins in RAW 264.7 mouse macrophages. RAW 264.7 cells were treated with compounds **1** (50 μM), **5** (12.5 μM), and **6** (50 μM) for 2 h and subsequently with LPS (1 μg/mL) for 4 h. (A) Representative western blots for NF-κB p65, I-κBα, IKKα/β, iNOS, COX-2, and glyceraldehyde 3-phosphate dehydrogenase (GAPDH) protein expression. (B) Quantitative graph for P-NF-κB p65. (C) Quantitative graph for P-I-κBα. (D) Quantitative graph for P-IKKα/β. (E) Quantitative graph for iNOS. (F) Quantitative graph for COX-2 (mean ± SD, *$p < 0.05$, **$p < 0.01$ compared to the group treated with 1 μg/mL pf LPS alone).

6 inhibited the production of IL-6 and TNF-α induced by LPS stimulation. Hence, they inhibited the initial stage of the inflammatory response stimulated by LPS. IκBα, an inhibitor of NF-κB activation, is phosphorylated by IKKβ. NF-κB isolated from IκB-α migrates to the nucleus and contributes to the expression of inflammatory genes.[19] In addition, NF-κB regulates the expression of iNOS and COX-2.[20] Therefore, we conducted western blotting to examine whether compounds **1**, **5**, and **6** inhibited the expression of NF-κB, IκBα, IKKα/β, iNOS, and COX-2. Compounds **1**, **5**, and **6** inhibited iNOS and COX-2 expression by inhibiting the NF-κB/I-κBα pathway. Based on the biological data of the isolated compounds, β-resorcylic acid lactones with a ketone group at C-9 position were more active than those with hydroxyl groups. In addition, two double bonds at C-10/C-11 and C-14/C-15 seem to affect the better activity, as shown in compounds **5** and **6**. In conclusion. Compounds **1**, **5**, and **6** demonstrated the potential to effectively induce anti-inflammatory activity by inhibiting the synthesis of pro-inflammatory cytokines.

EXPERIMENTAL SECTION

General Experimental Procedures. Optical rotations were measured at room temperature with a JASCO P-2000 polarimeter (JASCO, Easton, PA) using a 1 cm cell. The infrared (IR) spectra were recorded using an Agilent Cary 630 FTIR spectrometer (Agilent Technologies, Santa Clara, CA). High-resolution electrospray ionization mass spectrometry (HRESIMS) data were acquired using a UHR electrospray ionization quadrupole time-of-flight (ESI Q-TOF) mass spectrometer (Bruker, Billerica, MA). Nuclear magnetic resonance (NMR) spectra were obtained using Varian NMR systems 500 MHz (^{1}H: 500 MHz, ^{13}C: 125 MHz) (Varian, Palo Alto, CA) with CD_3OD (Cambridge Isotope Laboratories, Inc., Tewksbury, MA).

Fungal Materials. The fungal strain (JS0419) was isolated from *S. japonica* Makino collected from a swamp in Suncheon, South Korea, in September 2011. The tissues of this plant were cut into small pieces (0.5 × 0.5 cm^2) and rinsed sequentially for 1 min with 2% sodium hypochlorite, 70% ethanol, and sterilized distilled water to remove external microorganisms. After air drying, the sterilized plant tissues were incubated on the malt extract agar (MEA) medium (4 g of yeast extract, 10 g of malt extract, 4 g of potato dextrose broth, and 18 g of agar per 1 L sterilized distilled water) with 50 ppm kanamycin, 50 ppm chloramphenicol, and 50 ppm Rose Bengal at 22 °C for 7 days. The actively growing fungus was transferred to the potato dextrose agar (PDA) medium (24 g potato dextrose broth and 18 g agar per 1 L of sterilized distilled water). The fungal strain was identified as *C. gloeosporioides* by Dr. Soonok Kim at National Institute of Biological Resources, South Korea based on the internal transcribed spacer (ITS) sequences. It was deposited as 20% glycerol stock in a liquid nitrogen tank at the Wildlife Genetic Resources Bank of the National Institute of Biological Resources (Incheon, Korea).

Mass Cultivation of the Fungus. The JS0419 strain was cultured on the solid PDA medium for 7 days at room temperature. Agar plugs were cut into small pieces (0.5 × 0.5 cm^2) under aseptic conditions and inoculated on a solid rice medium (60 g of rice, 90 mL of distilled water per 500 mL Erlenmeyer flasks). After incubation at room temperature for 30 days, 200 mL of ethyl acetate was added to each culture flask (50 × 500 mL Erlenmeyer flasks) followed by extraction for 1 day. They were then filtered to separate the supernatant from the solid mycelia. The supernatant was evaporated under reduced pressure at 35 °C to obtain the extract (110 g).

Extraction and Isolation. The crude extract (110 g) was fractionated by vacuum liquid column chromatography over silica gel using a stepwise gradient of *n*-hexane/acetone/MeOH (from 1:0:0, 60:1:0, 25:1:0, 7:1:0, 5:1:0, 4:1:0, 3:1:0, 2:1:0,

https://doi.org/10.1021/acsomega.2c07962
ACS Omega 2023, 8, 3530−3538

0:1:0, to 0:0:1) to obtain RM01−RM10 fractions. The RM6 fraction (1.65 g) was subjected to silica gel vacuum liquid column chromatography by elution with a gradient of $CHCl_3$/acetone to obtain subfractions RM6A to RM6J. Fraction RM6G (300 mg) was separated by C18 vacuum liquid column chromatography using a gradient of aqueous MeOH from 30 to 100% to obtain compounds **1** (4.6 mg), **7** (7.0 mg), and **8** (30 mg). The RM8 fraction (2.02 g) was separated by silica gel vacuum liquid column chromatography and eluted using a gradient of $CHCl_3$/acetone/MeOH (from 12:1:0, 10:1:0, 8:1:0, 7:1:0, 6:1:0, 5:1:0, 3:1:0, 1:1:0, 0:1:0, to 0:0:1) to obtain fractions RM8A to RM8L. Fraction RM8C (176 mg) was further separated into RM8C1-RM8C7 by C18 vacuum liquid column chromatography using a gradient of aqueous MeOH from 20 to 100%. Fraction RM8C5 (45 mg) was subjected to reverse-phase high-performance liquid chromatography (HPLC) (Phenomenex, Luna C18 (2), 5 μm, 250 mm × 10.0 mm, room temperature, 2.0 mL/min, isocratic 33% aqueous acetonitrile, UV 210 nm) to obtain compounds **9** (4.7 mg, t_R = 19 min), **10** (2.0 mg, t_R = 20.5 min), and **11** (2.9 mg, t_R = 16 min). Compounds **2** (3.0 mg, t_R = 35.5 min) and **4** (3.7 mg, t_R = 29.5 min) were isolated from RM8C6 (42 mg) using reversed-phase HPLC (Phenomenex, Luna C18 (2), 5 μm, 250 mm × 10.0 mm, room temperature, 2.0 mL/min, 60−80% aqueous MeOH, UV 210 nm). Fraction RM9G4 (33 mg) was purified by column chromatography using Sephadex LH-20, followed by reverse-phase HPLC (Phenomenex, Luna C18 (2), 5 μm, 250 mm × 10.0 mm, room temperature, 2.0 mL/min, 30−50% aqueous acetonitrile, UV 280 nm) to yield compounds **5** (2.0 mg, t_R = 36.0 min) and **6** (3.7 mg, t_R = 33.0 min). Fraction RM9G5 (75 mg) was subjected to reversed-phase HPLC (Phenomenex, Luna C18 (2), 5 μm, 250 mm × 10.0 mm, room temperature, 2.0 mL/min, 50−100% aqueous ACN, UV 210 nm) to obtain compound **3** (1.4 mg, t_R = 15 min).

Colletogloeopyrone A (1). Yellowish amorphous solid; $[\alpha]_D^{25}$ = +10.8 (c 0.1, MeOH); for ^1H and ^{13}C NMR data (500 MHz in CD_3OD), see Table 1; (+) HRESIMS m/z 343.1519 $[M + Na]^+$ (Calculated for $C_{18}H_{24}O_5Na$, 343.1516).

Colletogloeopyrone B (2). Yellowish amorphous solid; $[\alpha]_D^{25}$ = +2.7 (c 0.1, MeOH); for ^1H and ^{13}C NMR data (500 MHz in CD_3OD), see Table 1; (+)HRESIMS m/z 393.1078 $[M + Na]^+$ (Calculated for $C_{18}H_{23}ClO_6Na$, 393.1075).

Colletogloeolactone A (3). Yellowish amorphous solid; $[\alpha]_D^{25}$ = +5.5 (c 0.1, MeOH); for ^1H and ^{13}C NMR data (500 MHz in CD_3OD), see Table 2; (+)HRESIMS m/z 473.1787 $[M + Na]^+$ (Calculated for $C_{23}H_{30}O_9Na$, 473.1782).

Colletogloeolactone B (4). Yellowish amorphous solid; $[\alpha]_D^{25}$ = −4.7 (c 0.1, MeOH); for ^1H and ^{13}C NMR data (500 MHz in CD_3OD), see Table 2; (-)HRESIMS m/z 367.0952 $[M - H]^-$ (Calculated for $C_{18}H_{20}ClO_6$, 367.0954).

Conformational Search and DP4 Analyses for 1 and 4. Spartan's 18 performed conformational investigations on two candidates of **1** using the Molecular Mechanic Force Field (MMFF), which is based on molecular mechanics (Wavefunction, Irvine, CA). The density functional theory (DFT) method was used to further optimize conformers with a relative energy threshold of 10 kJ/mol in chloroform using the polarizable continuum model (PCM) model (Gaussian, Inc., Wallingford, CT). It produced 11 conformers for 17*S* diastereomers and 9 conformers for 17*R* diastereomers when the GIAO approach was applied at B3LYP/6-31G(d,p) using Gaussian 16 W and the Solvation Model Based on Density (SMD) solvent model. The Boltzmann distribution was used to average the conformer shielding tensors that were calculated. The Excel spreadsheet given by the original authors was used to apply the DP4+ analysis on the calculated shielding tensors. The same procedure was used to compute the shielding tensors of tetramethylsilane (TMS), a reference. The values of the GIAO magnetic shielding tensor were used to calculate chemical shifts.

For compound **4**, MacroModel (version 9.9, Schrödinger LLC) and Maestro (version 9.9, Schrödinger LLC) were used to perform a conformational search. Twenty-eight conformers for the 12*R* and 17*R* diastereomers were obtained using the Merck molecular force field (gas phase) with a 10 kJ/mol upper energy limit as the cutoff, 5 conformers for the 12*R* and 17*S* diastereomers, 10 conformers for the 12*S* and 17*R* diastereomers, and 35 conformers for the 12*S* and 17*S* diastereomers. Density functional theory (DFT) calculations using the TurbomoleX 4.3.2 program with the basis set def-SVP for all atoms and the functional B3-LYP were used to determine the shielding tensor values. The computed ^1H and ^{13}C chemical shift values were averaged using Boltzmann populations.

RAW 264.7 Cell Culture. RAW 264.7 cell line (American Type Culture Collection, Rockville, MD) was examined in this study. Dulbecco's modified Eagle's medium (Manassas, VA) supplemented with 10% fetal bovine serum (FBS) and 1% penicillin-streptomycin solution was used as the medium for cell culture. The cells were cultured at 37 °C in an atmosphere containing 5% CO_2.

Analysis of the Viability of RAW 264.7 Cells. The MTT assay was conducted to measure cytotoxicity. In a 96-well plate, 1×10^4 cells were dispensed per well and cultured for 24 h. After removing the supernatant, compounds **1**−**11** were treated at each concentration and cultivated for 24 h, and the absorbance of viable cells was measured at a wavelength of 450 nm using a spectrophotometer microplate (PowerWave XS; Bio-Tek Instruments, Winooski, VT).

Determination of the Production of Nitric Oxide (NO), Interleukin (IL)-6, and Tumor Necrosis Factor (TNF)-α. RAW 264.7 cells were seeded in a 96-well plate with 1×10^4 cells/well and after treating compounds **1**−**11** at each concentration. The cells were then treated with 1 μg/mL of lipopolysaccharide (LPS; Sigma-Aldrich, St. Louis, MO) for 24 h, and the supernatant was collected and mixed with the Griess reagent. NO production was measured at a wavelength of 540 nm using a spectrophotometer microplate, and the levels of IL-6 and tumor necrosis factor-α (TNF-α) were measured using an ELISA kit according to the guidelines of the manufacturer (BD Biosciences; San Diego, CA).

Quantitative Real-Time Reverse Transcription-Polymerase Chain Reaction (qRT-PCR). RAW 264.7 cells were treated with compounds **1**, **5**, and **6** and 1 μg/mL of LPS, lysed using an RNeasy mini kit (Qiagen, Valencia, CA), and total RNA purification was conducted according to the manufacturer's protocol. RNA was converted to complementary DNA (cDNA) using the RevertAid First Strand cDNA Synthesis Kit (Thermo Scientific, Madison, WI). The sense and antisense primers of each gene, which are specific to mice, are listed in Table S1.[21] PCR amplification was conducted using the Power SYBR Green PCR Master Mix (Applied Biosystems, Foster City, CA). Relative expression levels were calculated using real-time reverse transcription PCR based on the Quant 3 real-time PCR system (Applied Biosystems), and the $2-\Delta\Delta C_q$ method was applied by normalizing the expression using β-actin as the reference gene.

Western Blot Analysis. RAW 264.7 cells were cultured in a six-well plate at a density of 2×10^6 cells/well for 24 h. The cells

https://doi.org/10.1021/acsomega.2c07962
ACS Omega 2023, 8, 3530−3538

were then treated with **1**, **5**, **6**, and 1 μg/mL LPS and then lysed with radioimmunoprecipitation assay (RIPA) buffer supplemented with 1× protease inhibitor cocktail and 1 mM sodium orthovanadate (Na_3VO_4) phosphatase inhibitor. Cell extracts with the same amount of protein (10 μg/lane) were separated by 10% sodium dodecyl sulfate-polyacrylamide gel electrophoresis (SDS-PAGE) using the Pierce BCA protein analysis kit (Thermo Scientific). Proteins were electrophoresed on poly(vinylidene fluoride) (PVDF) membranes. Phosphonuclear factor-κB (NF-κB) p65, NF-κB p65, phospho-I-κBα (inhibitor of κBα), IκBα, phospho-IKKα/β, IKKα (IκB kinase α), IKKβ (IκB kinase β), inducible nitric oxide synthase (iNOS), and cyclooxygenase-2 (COX-2) were used as primary antibodies for each PVDF membrane, and secondary antibodies were used to label the target protein with glyceraldehyde 3-phosphate dehydrogenase (GAPDH) (Cell Signaling, Boston, MA). The combined antibodies were detected using Pierce ECL Advance western blotting detection reagents (Thermo Scientific) and visualized using a FUSION Solo Chemiluminescence System (PEQLAB Biotechnologie GmbH, Germany).

Statistical Analysis. All data are presented as the average values and standard deviation (SD). Statistical analyses were conducted using one-way analysis of variance (ANOVA) and Bonferroni's post-test to evaluate the differences among various experimental groups (GraphPad Prism 7.0, GraphPad Software, Inc., San Diego, CA). $p < 0.05$ and $p < 0.01$ were considered significant.

■ ASSOCIATED CONTENT

Supporting Information

The Supporting Information is available free of charge at https://pubs.acs.org/doi/10.1021/acsomega.2c07962.

NMR and MS spectra of compounds (PDF)

■ AUTHOR INFORMATION

Corresponding Authors

Ki Sung Kang − *College of Korean Medicine, Gachon University, Seongnam 13120, Republic of Korea;* orcid.org/0000-0003-2050-5244; Phone: +82-31-750-5402; Email: kkang@gachon.ac.kr

Sang Hee Shim − *Natural Products Research Institute, College of Pharmacy, Seoul National University, Seoul 08826, Republic of Korea;* orcid.org/0000-0002-0134-0598; Phone: +82 2 880 2479; Email: sanghee_shim@snu.ac.kr

Authors

Jaekyeong Kim − *Natural Products Research Institute, College of Pharmacy, Seoul National University, Seoul 08826, Republic of Korea*

Ji Yun Baek − *College of Korean Medicine, Gachon University, Seongnam 13120, Republic of Korea*

Sunghee Bang − *College of Pharmacy, Duksung Women's University, Seoul 01347, Republic of Korea;* orcid.org/0000-0002-6764-7373

Ji-Young Kim − *Department of Biomedical and Pharmaceutical Sciences, Graduate School, Kyung Hee University, Seoul 02447, Republic of Korea*

Yeongwoon Jin − *Natural Products Research Institute, College of Pharmacy, Seoul National University, Seoul 08826, Republic of Korea*

Jin Woo Lee − *College of Pharmacy, Duksung Women's University, Seoul 01347, Republic of Korea*

Dae Sik Jang − *Department of Biomedical and Pharmaceutical Sciences, Graduate School, Kyung Hee University, Seoul 02447, Republic of Korea;* orcid.org/0000-0001-5472-5232

Complete contact information is available at: https://pubs.acs.org/10.1021/acsomega.2c07962

Author Contributions

$^{\perp}$J.K., J.Y.B., and S.B. contributed equally to this work.

Notes

The authors declare no competing financial interest.

■ ACKNOWLEDGMENTS

This work was supported by the National Research Foundation (NRF) of Korea (NRF-2021R1A2C1004958 and NRF-2022R1A4A3022401).

■ REFERENCES

(1) Schulz, B.; Boyle, C.; Draeger, S.; Römmert, A.-K.; Krohn, K. Endophytic fungi: a source of novel biologically active secondary metabolites. *Mycol. Res.* **2002**, *106*, 996−1004.

(2) Winssinger, N.; Barluenga, S. Chemistry and biology of resorcylic acid lactones. *Chem. Commun.* **2007**, 22−36.

(3) Sugawara, F.; Kim, K.-W.; Kobayashi, K.; Uzawa, J.; Yoshida, S.; Murofushi, N.; Takahashi, N.; Strobel, G. A. Zearalenone derivatives produced by the fungus *Drechslera portulacae*. *Phytochemistry* **1992**, *31*, 1987−1990.

(4) Isaka, M.; Suyarnsestakorn, C.; Tanticharoen, M.; Kongsaeree, P.; Thebtaranonth, Y. Aigialomycins A− E, new resorcylic macrolides from the marine mangrove fungus *Aigialus parvus*. *J. Org. Chem.* **2002**, *67*, 1561−1566.

(5) Hellwig, V.; Mayer-Bartschmid, A.; Müller, H.; Greif, G.; Kleymann, G.; Zitzmann, W.; Tichy, H.; Stadler, M. Pochonins A− F, new antiviral and antiparasitic resorcylic acid lactones from *Pochonia chlamydosporia* var. *catenulata*. *J. Nat. Prod.* **2003**, *66*, 829−837.

(6) Xu, L.; Xue, J.; Zou, Y.; He, S.; Wei, X. Three new β-resorcylic acid lactones from *Paecilomyces* sp. SC0924. *Chin. J. Chem.* **2012**, *30*, 1273−1277.

(7) Bang, S.; Lee, C.; Kim, S.; Song, J. H.; Kang, K. S.; Deyrup, S. T.; Nam, S. J.; Xia, X.; Shim, S. H. Neuroprotective glycosylated cyclic lipodepsipeptides, Colletotrichamides A-E, from a halophyte-associated fungus, *Colletotrichum gloeosporioides* JS419. *J. Org. Chem.* **2019**, *84*, 10999−11006.

(8) Bang, S.; Kim, J.; Oh, J.; Kim, J. S.; Yu, S. R.; Deyrup, S.; Bahn, Y.; Shim, S. H. Rare β-resorcylic acid derivatives from a halophyte-associated fungus *Colletotrichum gloeosporioides* JS0419 and their antifungal activities. *Mar. Drugs* **2022**, *20*, No. 195.

(9) Smarun, A. V.; Duzhin, F.; Petković, M.; Vidović, D. Alkene-assisted cis-to-trans isomerization of non-conjugated polyunsaturated alkenes. *Dalton Trans.* **2017**, *46*, 14244−14250.

(10) Kusumi, T. Determination of the absolute configuration of organic compounds by means of NMR spectroscopy. *J. Synth. Org. Chem., Jpn.* **1993**, *51*, 462−470.

(11) Smith, S. G.; Goodman, J. M. Assigning the stereochemistry of pairs of diastereoisomers using GIAO NMR shift calculation. *J. Org. Chem.* **2009**, *74*, 4597−4607.

(12) Smith, S. G.; Goodman, J. M. Assigning stereochemistry to single diastereoisomers by GIAO NMR calculation: The DP4 probability. *J. Am. Chem. Soc.* **2010**, *132*, 12946−12959.

(13) Grimblat, N.; Zanardi, M. M.; Sarotti, A. M. Beyond DP4: an improved probability for the stereochemical assignment of isomeric compounds using quantum chemical calculations of NMR shifts. *J. Org. Chem.* **2015**, *80*, 12526−12534.

(14) Lodewyk, M. W.; Siebert, M. R.; Tantillo, D. J. Computational prediction of ^{1}H and ^{13}C chemical shifts: a useful tool for natural

product, mechanistic, and synthetic organic chemistry. *Chem. Rev.* **2012**, *112*, 1839−1862.
(15) Pospíšil, S.; Sedmera, P.; Halada, P.; Petricek, M. Extracellular carbohydrate metabolites from *Streptomyces coelicolor* A3(2). *J. Nat. Prod.* **2007**, *70*, 768−771.
(16) Cochrane, R. V.; Sanicher, R.; Lambkin, G. R.; Reiz, B.; Xu, W.; Tang, L.; Vederas, J. C. Identification and reconstitution of the polyketide synthases responsible for biosynthesis of the antimalarial agent, cladosporin. *Angew. Chem., Int. Ed.* **2016**, *55*, 664−668.
(17) Xu, R.; Li, X. M.; Wang, B. G. Penicisimpins A-C, three new dihydroisocoumarins from *Penicillium simplicissimum* MA-332, a marine fungus derived from the rhizosphere of the mangrove plant *Bruguiera sexangula* var. *rhynchopetala*. *Phytochem. Lett.* **2016**, *17*, 114−118.
(18) Minnich, D. J.; Moldawer, L. L. Anti-cytokine and anti-inflammatory therapies for the treatment of severe sepsis: progress and pitfalls. *Proc. Nutr. Soc.* **2004**, *63*, 437−441.
(19) Nguyen, T.; Sherratt, P. J.; Huang, H.-C.; Yang, C. S.; Pickett, C. B. Increased protein stability as a mechanism that enhances Nrf2-mediated transcriptional activation of the antioxidant response element. Degradation of Nrf2 by the 26S proteasome. *J. Biol. Chem.* **2003**, *278*, 4536−4541.
(20) Goppelt-Struebe, M. Molecular mechanisms involved in the regulation of prostaglandin biosynthesis by glucocorticoids. *Biochem. Pharmacol.* **1997**, *53*, 1389−1395.
(21) Trinh, T. A.; Park, J.; Oh, J. H.; Park, J. S.; Lee, D.; Kim, C. E.; Choi, H.; Kim, S.; Hwang, G. S.; Koo, B. A.; Kang, K. S. Effect of herbal formulation on immune response enhancement in RAW 264.7 macrophages. *Biomolecules* **2020**, *10*, No. 424.

https://doi.org/10.1021/acsomega.2c07962
ACS Omega 2023, 8, 3530−3538